Influence of dominant salts on the removal of trace micropollutants by hollow fiber nanofiltration membranes

Sam B. Rutten [a,b], Moritz A. Junker [a], Lucía Hernández Leal [b], Wiebe M. de Vos [a], Rob G.H. Lammertink [a], Joris de Grooth [a,c,*]

[a] *Membrane Science and Technology, University of Twente, MESA+ Institute for Nanotechnology, P.O. Box 217, 7500 AE, Enschede, The Netherlands*
[b] *Wetsus, European Centre of Excellence for Sustainable Water Technology, Oostergoweg 9, 8911 MA, Leeuwarden, The Netherlands*
[c] *NX Filtration BV, Josink Esweg 44, 7545 PN Enschede, The Netherlands*

ARTICLE INFO

ABSTRACT

Nanofiltration (NF) is seen as a promising advanced treatment technology to deal with the increasing concentration of micropollutants (MPs) in water sources globally. To further improve the successful implementation of NF, an increased understanding of membrane transport mechanisms is important. One key aspect among these mechanisms concerns the influence of solution composition on the overall filtration performance. Although several studies report the influence of feed solution composition on the removal of micropollutants by NF membranes, the underlying mechanisms are often not fully understood. In this study, the impact of dominant salts (NaCl, Na_2SO_4, $MgCl_2$) on the removal of trace MPs by commercial hollow fiber NF membranes (dNF40, dNF80) was investigated. Common conditions where salt concentrations greatly exceed MP concentrations were applied to assess their potential influence at environmentally relevant concentrations. Experimental observations reveal that a dominant salt alters MP transport behaviour substantially. The impact of a dominant salt on MP transport via electrostatic coupling increases for MPs of higher mobility inside the membrane. Overall, higher mobility, i.e. lower removal, of MPs through the dNF80 membranes was observed. Correspondingly, the strongest impact was observed for the dNF80 membrane, where the removal of positively charged atenolol increased from about 60% to >90% in the presence of Na_2SO_4. A theoretical transport model (DSPM&DE) was used to assist the interpretation of experimental observations further. Model predictions reveal the relevance of two effects: the influence of a dominant salt on the charge-based membrane properties and the electrostatic coupling in the form of the arising membrane potential.

1. Introduction

For several decades [1], micropollutants (MPs) have been detected in the majority of water bodies, typically in the concentration range of ng L^{-1} to μg L^{-1} [2–6]. These contaminants consist of anthropogenic substances originating from, amongst others, the use of pharmaceutical and personal care products, agriculture, and industries [6]. Uncertainties regarding long-term exposure and potential synergistic effects of MP mixes on human health and the environment have raised considerable concerns [7]. Furthermore, with an ever-increasing variety and quantity of these compounds detected in many water bodies, the presence of MPs has become an urgent problem to address [6,8–13].

Simultaneously, as water scarcity is increasing globally due to population growth, socio-economic development, and climate change, there is a growing need for sustainable solutions for the long-term supply of potable water. In this context, wastewater reclamation, where water treatment facilities extensively treat wastewater for reuse, has been identified as one viable source of drinking water [14–16].

Most conventional treatment technologies cannot adequately remove potentially hazardous MPs from (waste)water streams. To mitigate the pollution of surface- and groundwater sources from wastewater effluent while simultaneously increasing the potable water supply, current treatment systems need to be complemented or replaced by more advanced treatment techniques.

One promising advanced treatment system to retain MPs is the implementation of high-pressure membrane filtration processes, such as nanofiltration (NF) or reverse osmosis (RO) [17–21]. Since NF processes require less energy than RO while still removing certain small organic molecules such as naproxen up to >95 %, NF is considered the

economically favourable and sustainable option [22]. The viability of NF membranes as an advanced method in wastewater treatment has already been shown in multiple studies [21,23–27], and optimisation of these membranes for this specific application is an ongoing field of research [28–33].

NF exhibits unique separation properties that offer many potential benefits in water treatment. Due to the relatively low molecular weight cut-off (MWCO) of 200–1000 Da, small uncharged solutes can effectively be retained, while ions are partially retained based on their sign and magnitude of charge [34,35]. Many studies evaluated the applicability of NF membranes for MP removal [26,29,31,33,36–40]. In these studies, MP removal of single pollutants, or mixtures, was determined while not considering the presence of background solutes. However, in natural water sources and wastewater, the feed solution composes of a mixture of solutes, which allows for solute–solute and specific solute–membrane interactions [41–44]. These specific interactions can substantially alter the transport through NF membranes [27, 45–48]. Consequently, predicting removal in real water streams is still challenging and often limited to specific process conditions [49–51].

Some research has focused on the performance of NF membranes to remove MPs from spiked drinking water sources [45,48,52,53]. These studies showed the potential of NF as a complementary process in water treatment. However, knowledge regarding the mechanisms of retention is currently still lacking [54]. A theoretical understanding of underlying separation mechanisms is required to improve the removal of MPs using NF membranes and enable the prediction of full-scale applications.

A substantial amount of work has been performed which demonstrates the influence of fouling [27,46–48,55], ionic strength [48,56] (in the form of NaCl) and the presence of (divalent) cations (in the form of calcium) [46,48,56,57] on MP transport. These previous studies highlight the importance of considering the influence of water matrix on MP removal and its direct implications for application. However, one important open question that relates to the influence of the water matrix on MP removal is the specific influence of ions, including both monovalent and divalent anions and cations, on the removal of MPs. Previous research has shown that dominant salts, i.e. salts at significantly higher concentrations, can affect the removal of trace ions during NF of ionic mixtures [58,59]. In these studies, it was shown that the rejection of a dominant salt by NF membranes results in the development of a spontaneous electric field to comply with the zero-current condition in a steady state. The electric fields can either accelerate or retard trace-ions influencing their removal. Since MPs are typically observed at trace concentrations in water bodies, it can be assumed that the presence of different dominant ions will similarly affect the removal of charged MPs.

In this work, we investigate the effects of dominant salt ions on the transport of MPs through NF membranes. To reach this goal, the effect of NaCl, MgCl$_2$, and Na$_2$SO$_4$ at increasing ionic strengths on the retention of a mix of four MPs was investigated. Two commercial, hollow fiber NF membranes based on polyelectrolyte multilayers were used. The experimental results are interpreted through a theoretical transport model. The modelled results provide an understanding of the extent to which electric potential gradients caused by dominant ions influence the transport behaviour of MPs. We show that the removal of charged MPs can be majorly affected by the presence of a single, dominant salt. The transport model confirms the major influence of the dominant salt. Two underlying mechanisms are suggested: the electric coupling to ion transport via induced filtration potential and the influence of ionic solution composition on the effective membrane charge.

2. Materials and methods

2.1. Chemicals and membranes

Experiments were performed using two lab scale modules with NF membranes (dNF40, dNF80) obtained from NX Filtration (Enschede,

Table 1
Characteristics of the hollow fiber polyelectrolyte multilayer membranes provided by NX Filtration.

Membrane	dNF40	dNF80
MWCO [Da][a]	400	800
Membrane surface area [m^2][a]	0.065	0.065
Permeability [L m^{-2} h^{-1} bar^{-1}][b]	6.1 ± 0.1	7.2 ± 0.1
pH range [operation][a]	2–12	2-12
pH range [cleaning][a]	1–14	1-13

[a] Information provided by supplier.
[b] Determined at increasing TMP; T=20 °C

The Netherlands). Table 1 provides the technical specification of the membranes and modules used in this study.

All chemicals were of analytical grade and were obtained from Sigma-Aldrich (Zwijndrecht, The Netherlands). Atenolol, atrazine, sulfamethoxazole, and naproxen were selected as MPs of interest due to their charge at a neutral pH, and known occurrence in secondary treated wastewater effluent [6,60]. Furthermore, the MPs were selected based on their molecular weight, which was low enough to allow some passage based on the MWCO of the studied membranes and high enough for accurate analysis with the equipment used. The physicochemical properties of the four selected MPs in this study are listed in Table 2. The diffusion coefficient of the MPs was estimated using the Wilke-Chang correlation [61]:

$$D_S = 7.4 \cdot 10^{-12} \frac{(x M_W)^{0.5} T}{\eta V_M^{0.6}} \tag{1}$$

Here, D_S is the diffusion coefficient of the solute [m^2 s^{-1}], x is the association parameter (2.6 for water), M_W is the molecular weight of water [18.02 g mol^{-1}], T is the temperature [293 K], η is the viscosity of water at 20 °C [1 Pa s] and V_M is the molecular volume of the solute [cm^3 mol^{-1}]. This correlation has frequently been used to estimate diffusion coefficients for MPs in literature [25,39,62] and is expected to give a reasonable estimate since the conditions and solute properties of the current study are well within the range studied by Wilke and Chang [61]. Before the experiments at a low concentration of MPs (35 μg L^{-1}), a combined stock solution of 3.5 mg L^{-1} of each MP in demineralised water was prepared and was stored at 5 °C in the dark. Feed solutions at high concentrations of MPs (i.e. 3 mg L^{-1} of each MP) were prepared directly before each experiment.

2.2. Experimental protocol

All experiments were performed using a Mexplorer bench-scale test unit obtained from NX Filtration. This test unit consists of lab-scale membrane module headers, which are fed with a vane pump. Feed flow and transmembrane pressure were controlled using manual needle valves. All experiments were performed at a constant temperature (20 ± 0.5 °C) using a heat exchanger connected to the feed. The concentrate and permeate were fully recirculated to the feed tank to limit any concentration effects during the experiments. A schematic overview of the experimental setup is provided in SI1. Prior to the experiments, both membrane modules were flushed with approximately 120 liters of demineralised water to remove preservatives. Following this flush, feed solutions, without the addition of salt ions, were recirculated for 24 h, which was found sufficient to ensure saturation of the membrane surface and steady-state passage of the selected MPs (also observed by [26,56]). After initial filtration measurements at a concentration of 3 mg L^{-1} of each MP, additional measurements at a concentration of 35 μg L^{-1} of each MPs were performed with the dNF40 membrane, as will be explained later on. Initial feed concentrations were selected to allow for the analytic determination of a 1 % passage of the MPs of interest (see 2.3). For measurements in the μg L^{-1} range, the feed solution was recirculated at a constant flux of 20 ± 2 L m^{-2} h^{-1}

Table 2
Physicochemical properties of the studied MPs.

	Atenolol	Atrazine	Sulfamethoxazole	Naproxen
Chemical formula	$C_{14}H_{22}N_2O_3$	$C_8H_{14}ClN_5$	$C_{10}H_{11}N_3O_3S$	$C_{14}H_{14}O_3$
Molecular weight M_W [g mol^{-1}]	266.34	215.68	253.28	230.26
pKa[a] [–]	9.4	2.3	1.4;5.8	4.8
Molar volume[a] V_M [cm^3 mol^{-1}]	236.6	169.8	173.1	192.2
Diffusion coefficient[b] D_S [10^{-10} m^2 s^{-1}]	5.58	6.81	6.73	6.32
Charge at experimental pH	+	0	−	−
Application	β-Blocker	Herbicide	Antibiotic	Anti-inflammatory

[a]Adopted from SciFinder.

[b]From Wilke-Chang correlation (see Eq. (1)).

Table 3
Ionic strength and corresponding molar concentration.

Ionic strength [mmol/L]	Na$_2$SO$_4$ [mmol/L]	NaCl [mmol/L]	MgCl$_2$ [mmol/L]
0	0	0	0
15	5	15	5
30	10	30	10
60	20	60	20

for an extended period of 72 h before sampling to account for MP adsorption to the membrane surface area and ensure steady-state MP passage [30,48,56]. Cross-flow velocity was kept constant at 0.6 m s^{-1} unless otherwise stated. This cross-flow velocity was chosen based on a previous study to limit the influence of concentration polarisation [63] while remaining in a range relevant to industrial applications. Samples were taken from the permeate and feed, and the passage P (%) of the solutes was calculated using

$$P = \frac{C_p}{C_b} * 100\% = (1 - R) \tag{2}$$

Where C_p and C_b are the permeate and feed bulk concentration (mol m^{-3}), respectively, and R (%) is the retention. Although solute retention is more commonly applied, we choose passage to evaluate membrane performance since it is directly proportional to the solute permeate concentration, which is more relevant for practical purposes. Furthermore, passage allows for a more direct comparison of the influence of ions on the MP flux through the selected membranes.

After sampling, the salt concentration was adjusted to the ionic strengths indicated in Table 3 by the addition of either NaCl, MgCl$_2$ or Na$_2$SO$_4$. Following the salt addition, the flux was readjusted to 20 ± 2 L m^{-2} h^{-1} and another 24 h of stabilisation was provided before sampling.

The same dNF80 and dNF40 membrane modules were used throughout the experiments. To remove residual ions and MPs from the setup, the module was flushed with demineralised water between each experiment. Flushing continued until the conductivity of the feed, permeate and concentrate were comparable to the initial conductivity of demineralised water. For measurements at a high concentration of MPs, the membranes were additionally cleaned using a 400 ppm sodium hypochlorite solution. Each experiment was performed at least three times.

2.3. Analytical methods

Samples at high MP concentration (Feed ∼ 3 mg L^{-1}) were analysed using an UHPLC (Dionex Ultimate 3000) with an Acclaim™RSLC 120 C18 column (particle size 2.2 um, pore size 120 Å, 2.1 × 100 mm, Thermo Scientific), and a UV/Vis detector (225 nm).

Analysis of MPs at a feed concentration of ∼35 μg L^{-1} was performed using an Agilent 6420 triple quadrupole liquid chromatography mass spectrometer (LC/MS) (Agilent Technologies, Amstelveen, The Netherlands). Before analysis, samples were pretreated using 50 μ L of modifier (0.265 M NH$_3$, 0.02 M C$_2$H$_2$O$_4$ and 3.40 M CH$_2$O$_2$) and 50 μ

L of internal standard and directly injected. Analytes were separated using an Agilent Zorbax Eclipse Plus C18 RRHD column with a UHPLC guard Zorbax Eclipse Plus C18 pre-column.

Details regarding the eluent and gradient profiles of both methods, and the MS/MS settings, are provided in SI1.

Salt passage was determined using direct electrical conductivity measurements of both the feed and permeate using a Mettler Toledo SevenExcellence pH/Conductivity meter (Tiel, The Netherlands), with a nominal range of 0–1000 S cm^{-1} and accuracy of 0.5 % of the measured value.

2.4. Membrane characterisation

Experiments were performed to determine the pure water permeability, PEG retention and ternary ion retention which are required to characterise the membrane properties for the theoretical transport model. During characterisation, the cross-flow velocity was kept constant at 0.6 m s^{-1}, and the temperature was controlled to $20 \pm 0.5\,^\circ$ C. Each experiment was performed at least three times.

Pure water permeability A (L m^{-2} h^{-1} bar^{-1}) was determined by measuring water flux J (L m^{-2} h^{-1}) at feed pressures Δp (bar) ranging from 1 to 6 bar.

$$A = \frac{J}{\Delta p} \tag{3}$$

Here, the water flux J was calculated based on permeate mass m_p (kg) as a function of permeation time t (h), using the density of water ρ (1 kg L^{-1}) and the active membrane area A$_m$ (0.065 m^2).

$$J = \frac{m_p}{\rho A_m t} \tag{4}$$

To evaluate the effect of operational settings on MP passage, the solute permeability B (m s^{-1}) of a select set of experiments was determined using

$$B = \frac{P \cdot (J/3.6 \cdot 10^6)}{exp((J/3.6 \cdot 10^6)/k_{c,i}) \cdot (1 - P)} \tag{5}$$

Where $k_{c,i}$ (m s^{-1}) is the solute mass transfer coefficient determined using the Sherwood relationship as provided in SI2.

To evaluate steric exclusion of uncharged solutes, passage of polyethylene glycol (PEG) of different molecular weights (62 106, 200, 400 g mol^{-1}) was measured at three feed pressures (2, 4, and 6 bar). Passage was calculated based on Eq. (2). Concentrations of PEG in both feed and permeate were determined using gel permeation chromatography, as described in [64].

Charge-based exclusion was evaluated by measuring the passage of ternary ion mixtures at a pressure of 4 bar. Here, mixtures of MgCl$_2$ + NaCl and Na$_2$SO$_4$ + NaCl in molar ratios of the non-common ions 1:3, 1:1 and 3:1 were used. Passage was calculated based on Eq. (2). The concentration of individual ions was determined using ion chromatography (IC). The IC setup (858 Professional Sample Processor, 2x Eco IC, Metrohm) consisted of an anion column (Metrosep A Supp 17 - 150/4.0), a suppressor for the anion analysis (MSM Rotor A), and a cation column (Metrosep C 6 - 150/4.0). The eluent consisted of an 4 mM NO$_3$ solution and a 5 mM Na$_2$CO$_3$ + 0.2 mM NaHCO$_3$ solution

for the cation and anion column, respectively. Flow rates were set to 0.6 mL min^{-1} in the cation column, while the anion column was fed at 0.9 mL min^{-1}. Alongside the eluent, a suppressor solution of 0.3 M H$_3$PO$_4$ was used.

3. Theoretical transport model

In this study, we applied the frequently used Donnan Steric Pore Model and Dielectric Exclusion (DSPM&DE) model [65–68], in which the transport through the separation layer of the membrane is described by the extended Nernst–Planck equation. The partitioning at the membrane surface is determined by Donnan, dielectric (Born model), and steric exclusion. We applied two extensions to the model to cover the relevant physical phenomena for MP transport through an NF membrane.

First, we introduced an additional term accounting for the affinity between MPs and the membrane proposed by Verliefde et al. [69], as it was shown that for uncharged MPs steric hindrance alone often underpredicts the passage [49,62]. This affinity term also accounts for potential differences in the activity of MPs between the membrane phase and water phase, which we could not predict at this point. Further equilibrium partitioning studies are required to understand this effect. Secondly, we introduced a log-normal distribution for pore size. We refer to our previous work for more detailed information on the fitting procedure [64].

The full set of equations is shown in SI2. The model was solved in MATLAB using the algorithm presented by Geraldes et al. [70].

4. Results and discussion

As mentioned in Section 2.2, results are presented in terms of salt or MP passage. While retention is most commonly used to represent the performance of NF membranes, it was decided to use passage as this more directly relates to the transport of solutes through the membrane. By doing so, differences in the passage of MPs due to dominant ions can more easily be interpreted as increased or decreased solute flux.

We divide this section into four parts. In the first three parts, we present and discuss the experimental observations of: passage of dominant salts in the presence of trace MPs, passage of trace MPs in the absence of salt, passage of trace MPs in the presence of salt. In the last part, the DSPM-DE model is used to analyse experimental results in more depth and to establish a more fundamental understanding of the transport mechanisms.

4.1. Ion passage at increasing ionic strength

Ion passage in the presence of MPs through both membranes was determined using conductivity probes. Since the MPs were present at trace concentrations, i.e. MP-to-salt concentration ratios of at least 1:250, the influence of charged MPs on conductivity was assumed to be insignificant. Due to the very small relative amount of MPs, the influence on the passage of ions is considered negligible. Fig. 1 presents the observed passage of the selected dominant salts at increasing ionic strength.

For the dNF80 membrane, an average passage of sodium sulphate and magnesium of respectively ∼5% and ∼50%, irrespective of ionic strength, was observed. Sodium chloride passage was significantly higher, ranging from 89 ± 0.4% at 15 mM to 94 ± 0.2% at 60 mM. Since it is known that monovalent ions more efficiently pass through NF membranes, the observed results were in line with the expectations. Furthermore, the limited influence of ionic strength in the current study matched well with previously reported results [63].

The passage of all salts through the dNF40 membrane remained stable irrespective of the ionic strength of the feed solution (Fig. 1). Approximate passages of 88%, 7% and 16% for NaCl, Na$_2$SO$_4$, and MgCl$_2$, rsespectively, were observed. Based on these observations, it is

suspected that the influence of ionic strength on salt passage through both membranes has minimal effect in the currently studied range. Salt passages indicate charged-based exclusion mechanisms and can be used to qualitatively compare the properties of the dNF80 and dNF40 membranes. The low passage of Na$_2$SO$_4$ (∼5%) in combination with a relatively high passage of MgCl$_2$ (∼50%) observed for the dNF80 indicates a significant contribution of Donnan exclusion for ion passage. Simultaneously, the high passage of NaCl (∼90%) indicates a substantial contribution of dielectric exclusion towards the transport of ions. Therefore, based on the current observations, it is suggested that both charge-based exclusion mechanisms (i.e. Donnan and dielectric exclusion) substantially contribute towards the transport through the dNF80 membrane. For the dNF40 membrane, both Na$_2$SO$_4$ and MgCl$_2$ passage remained low (<20%), while NaCl passage was similarly high as seen for the dNF80 (∼90%). These observations suggest that Donnan exclusion minorly influences ion passage for the dNF40 membrane and that dielectric exclusion mechanisms mainly govern the transport.

4.2. MP passage in pure water

Micropollutant passage through both the dNF80 and dNF40 membranes was determined at the higher feed MP concentrations (∼3 mg L^{-1}). Throughout the experiments, the pH was not controlled, as this prevented the addition of ions to the feed solution. Each experiment continuously monitored pH, which remained relatively stable around 6.6 ± 0.2. At this pH, sulfamethoxazole and naproxen are negatively charged, atenolol is positively charged, and atrazine remains neutral.

Firstly, an overall relatively low passage of the selected MPs was observed considering their molecular weights, ranging between 200 and 300 g mol^{-1}, with respect to the MWCOs of 800 (dNF80) and 400 (dNF40) Dalton provided by the supplier (Table 1). This low passage, relative to the reported MWCO, can have multiple causes. The MWCO is typically measured with standardised molecules (such as PEG), which likely have a different affinity towards the membrane material. Furthermore, the passage could be influenced by the shape of molecules. Additionally, the influence of charge-based exclusion of molecules is typically not considered. Lastly, it can be assumed that the MWCO values given by the supplier include a certain safety margin.

Consistently higher passage of MPs was observed for the dNF80 membrane when compared to the dFN40. Overall, the dNF80 most efficiently retained naproxen by, on average, 20 ± 2%. Following naproxen, an increasing passage of sulfamethoxazole (34 ± 2%), atenolol (36 ± 5%) and atrazine (55 ± 1%) was observed. A clear trend in charge-based transport through the dNF80 was observed, in which negatively charged MPs (i.e. naproxen and sulfamethoxazole) showed the lowest passage, while neutral contaminants (i.e. atrazine) were transported most efficiently through the membrane. The low passage of negative MPs was in line with the suggested negative membrane charge, as observed in the salt passage measurements. Accordingly, atenolol, despite being the heaviest molecule, had higher passage values than both negatively charged MPs. Considering the molecular weights of the negatively charged MPs, a higher passage of naproxen (230.26 g mol^{-1}) over sulfamethoxazole (253.68 g mol^{-1}) was expected. Observations with both tested membranes (dNF80 & dNF40) show an opposite result, where naproxen passes less effectively than sulfamethoxazole. This result suggests that molecular weight and charge alone are insufficient to predict MP transport through the membrane effectively. Two potential alternatives we want to mention are the use of molecular volume to describe the molecular size and MP-membrane interactions. While sulfamethoxazole is a larger molecule based on molecular weight, its molecular volume is lower than that of naproxen (Table 2). Molecular volume could, therefore, potentially be a better representation of molecular size than molecular weight. Furthermore, solute-specific interactions with the membrane (sometimes referred to as hydrophobic interactions) could also result in unexpected trends in membrane passage. Limited passage of all
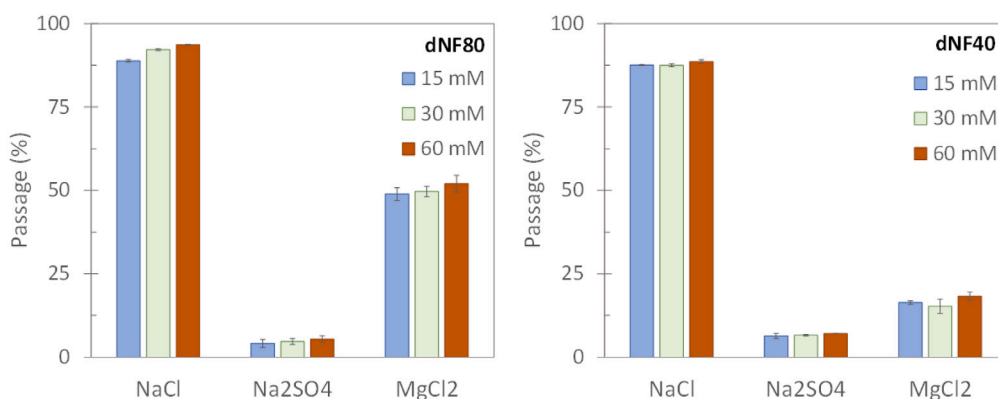
Fig. 1. Passage of NaCl, Na$_2$SO$_4$ and MgCl$_2$ through the dNF80 (left) and dNF40 (right), at the indicated ionic strengths. The error bars represent the standard error (dNF80: N=4; dNF40: N=3 for each salt and ionic strength).
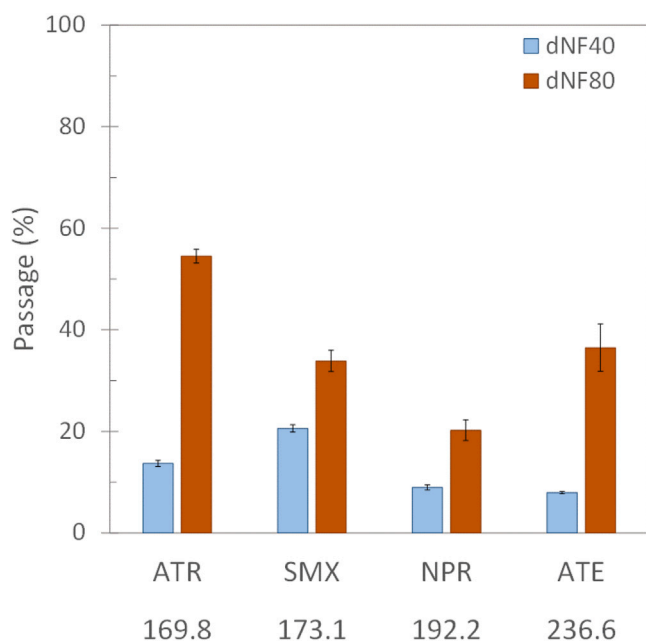

Fig. 2. MP passage by the dNF40 and dNF80 membranes at ∼0 mM ionic strength. Initial feed concentrations were set to 3 mg L^{-1}. SMX: sulfamethoxazole (−), NPR: naproxen (−), ATE: atenolol (+), ATR: atrazine (0). Molecular volumes of the MPs provided in cm^3 mol^{-1}. The error bars represent the standard error (dNF80: N=12; dNF40: N=9).

selected MPs, ranging between 8 ± 0.3% for atenolol and 21 ± 1% for sulfamethoxazole, through the dNF40 was observed (Fig. 2). The lower passages observed, combined with the limited difference between the selected MPs regarding charge, suggests a more substantial contribution of steric exclusion on passage as compared to the dNF80 membrane. Notably, the changed order of MP passage, compared to the dNF80 membrane, supports the minor influence of Donnan exclusion indicated in salt passage (see 4.1).

Due to the limited passage of the selected MPs through the dNF40 membrane, it was suspected that the effect of dominant salt species would be lessened. To increase the salt-to-MP ratio without altering the overall ionic strength of the feed solutions, filtration experiments with an initial MP concentration of 35 μg L^{-1} were performed. All experiments at the reduced MP concentration were performed with an increased cross-flow velocity (1 m s^{-1}). While this increase in cross-flow velocity could lead to changes in the observed passage, the effect is expected to be minor since concentration polarisation is limited within the currently applied operational conditions [63].

Passage of atrazine slightly reduced (∼−2%), and naproxen passage slightly increased (∼+2%), while no significant change in sulfamethoxazole and atenolol was observed (Fig. 3). No clear trend was observed in the minor changes in MP passage at the different concentrations. Therefore, it was expected that the decreased concentration would not affect the passage of MPs in a significant way. To determine if the slight difference in operational settings led to the change in the observed passage, the solute permeability of each MP at both concentrations was also determined (Fig. 3). Similar to the passage results, no trend in solute permeability was observed due to the reduced concentration. Therefore, it was presumed that the effect of operational conditions on MP passage was negligible in the studied regime. Since MPs are found in the high ng L^{-1} to low μg L^{-1} in environmental samples, it was decided to continue the experiments with the dNF40 membrane at environmentally relevant concentrations 35 μg L^{-1}. Furthermore, this reduced MP concentration would increase the salt-to-MP ratio, which was assumed to potentially enhance the proposed trace solute/dominant salt interactions throughout these experiments.

4.3. Change in MP passage due to the presence of dominant salt ions

This section presents experimentally observed passage of trace MPs in the presence of dominant salt and indicates potential underlying mechanisms. The next section utilises the theoretical transport model to perform a more detailed analysis of transport mechanisms.

4.3.1. dNF80

The presence of sodium chloride increased the passage of the charged MPs (i.e. sulfamethoxazole, naproxen and atenolol) (Fig. 4). Previous research has proposed electrostatic screening, changes in the solute-to-pore size ratio and solute dehydration as potential mechanisms leading to increased passage [71,72]. Electrostatic screening of the membrane charge would lead to opposite trends in positively charged (i.e. atenolol) and negatively charged (i.e. naproxen and sulfamethoxazole) MP passage, which was not observed and is therefore unlikely the reason. No significant changes in atrazine and PEG passage in the presence of sodium chloride were observed (Figs. 4 and SI3). Based on this observation, it was presumed that changes to the pore size were insignificant. Since both electrostatic screening and pore swelling are unlikely explanations for the observed trend, solute dehydration of the charged micropollutants is the most likely mechanism. However, further in-depth analysis into the behaviour of atenolol, sulfamethoxazole, and naproxen is required to explain the observed changes in MP passage.

The presence of 60 mM Na$_2$SO$_4$ increased passage of sulfamethoxazole, from 34 ± 2% to 63 ± 8%. The increased passage indicates accelerated transport of sulfamethoxazole through the membrane, possibly due to electric coupling to ion transport [59]. Since divalent
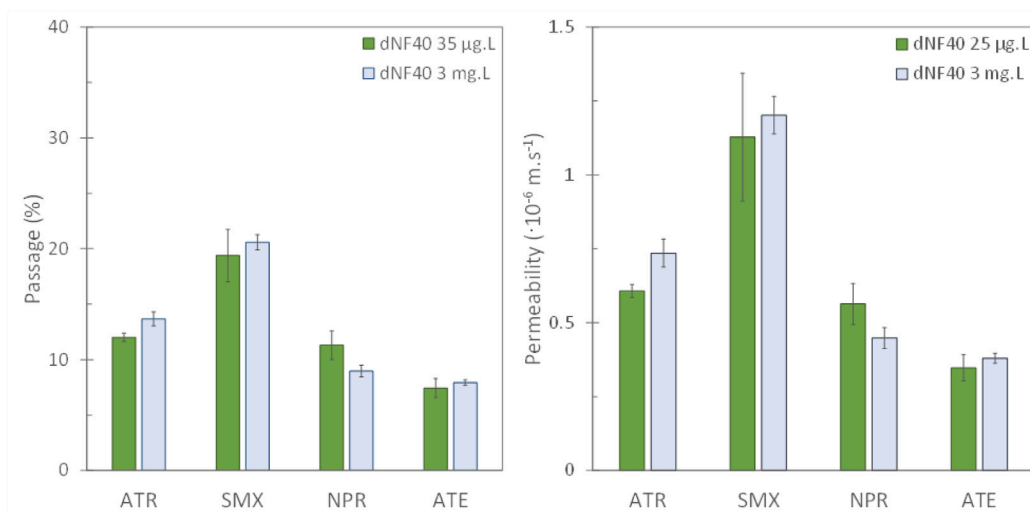
Fig. 3. MP passage and solute permeability through the dNF40 membrane at differing MP concentrations. SMX: sulfamethoxazole (−), NPR: naproxen (−), ATE: atenolol (+), ATR: atrazine (0). The error bars represent the standard error (N=9).
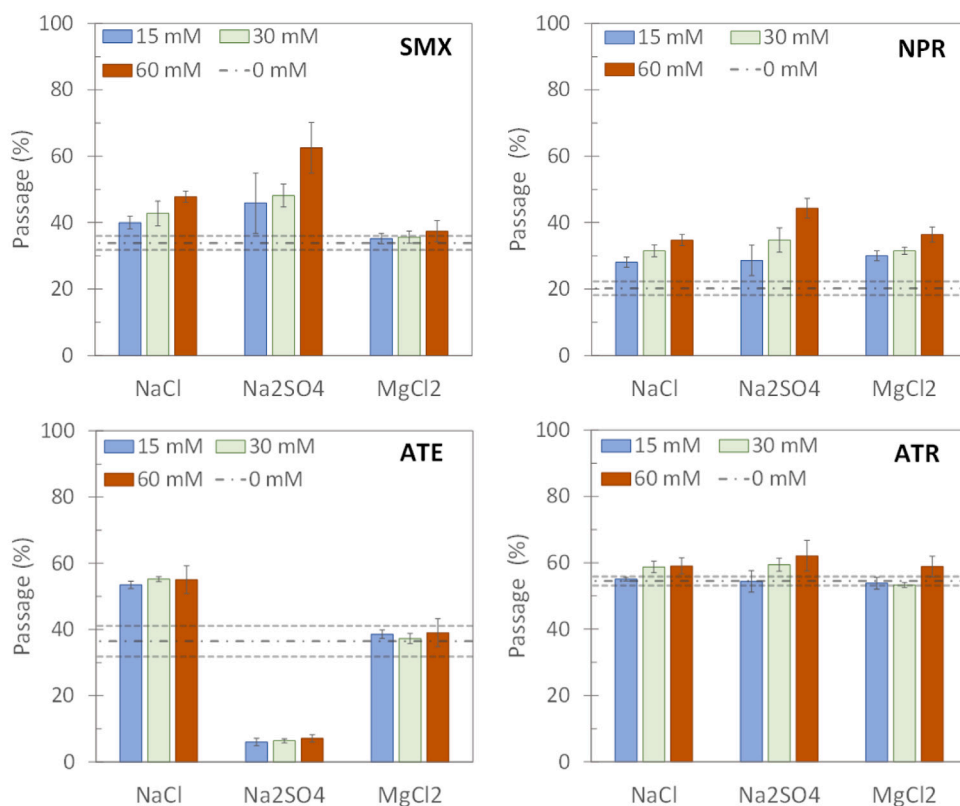

Fig. 4. Influence of increasing ionic strength on passage of MPs through dNF80 membranes. SMX: sulfamethoxazole (−), NPR: naproxen (−), ATE: atenolol (+), ATR: atrazine (0). The dotted and solid lines represent the average passage and the dashed lines represent the standard error, respectively. Error bars represent the standard error (N=4 for each salt).

anions, such as sulphate, are more strongly retained by the membrane than monovalent anions, improved transport of monovalent anionic solutes, such as sulfamethoxazole, could occur to maintain electroneutrality. Similarly, naproxen passage increased in the presence of Na_2SO_4, changing from 20 ± 2 to 44 ± 7%. While this could also be explained by the transmembrane electric field, the effect was less pronounced than for sulfamethoxazole. Based on the same mechanism, a decreased passage of cationic solutes, such as atenolol, would occur. This effect was clearly observed (Fig. 4), as passage of atenolol decreased from

36 ± 5% to 7 ± 1% in the presence of Na_2SO_4. These observations support the potential occurrence of ion transport induced electric fields described by Yaroshchuk [73] and Pages et al. [59] when Na_2SO_4 is present as a dominant salt species. Lastly, only a slight increase in atrazine passage of ~7% was observed with increasing Na_2SO_4 concentration (Fig. 4). A high passage of atrazine (~55%) in the absence of dominant salt species was previously observed. Due to this relatively high passage, it was expected that any potential effects of dominant ions on passage would be much larger compared to similar
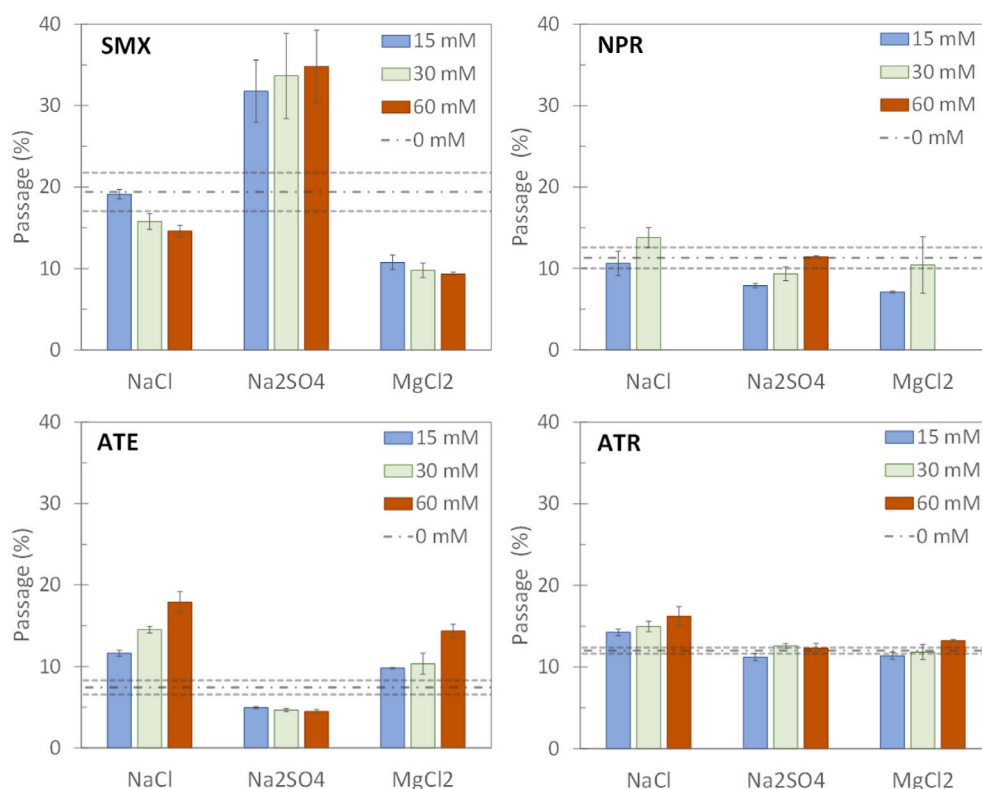
Fig. 5. Influence of increasing ionic strength on passage of MPs through dNF40 membranes. SMX: sulfamethoxazole (−), NPR: naproxen (−), ATE: atenolol (+), ATR: atrazine (0). The dotted and solid lines represent the average passage and standard error, respectively. Error bars represent the standard error (N=3 for each salt).

effects on the other MPs selected. As shown in Fig. 4, the change in atrazine passage was much smaller compared to the changes observed for the other selected MPs. We attribute the steady increase of passage with ionic strength to increased osmotic pressure leading to lower membrane flux (measurements of the dNF80 module were performed at constant transmembrane pressure). Considering this observed limited change in atrazine passage, it is expected the passage of neutral trace contaminants through dNF80 membranes is not affected by different salts and their respective concentration.

Since a relatively high passage of magnesium chloride through the dNF80 membrane was observed (∼50%), a limited impact on the passage of MPs was expected. This was reflected in the results, where no significant change in passage of sulfamethoxazole, atenolol and atrazine was observed at increasing ionic strengths of magnesium chloride. Therefore, solely based on experimental results, no specific effect of $MgCl_2$ on the passage of MPs through the dNF80 could be elucidated.

It must be noted that naproxen passage increased irrespective of the ion species used in the current study (Fig. 4). It was, therefore, not possible to elucidate the phenomena studied in the current research based on these results. Further research into the specific interactions of naproxen with different dominant ions is required to fully understand these results.

4.3.2. dNF40

The effect of dominant salt species on the passage of MPs through the dNF40 membrane was studied at lower MP concentration (∼35 µg L^{-1}) to increase the salt to MP ratios.

The permeate and feed concentration of naproxen at 60 mM ionic strength of magnesium chloride and sodium chloride decreased below the limit of quantification (∼0.1 µg L^{-1}). This decrease in feed and permeate concentration could be due to adsorption to the experimental setup. Naproxen is a relatively hydrophobic MP, with a Log K_{OW}

(octanol/water partition coefficient) of ∼3.18. Therefore, it potentially adsorbs to the (plastic) tubing of the experimental setup, leading to a significant decrease in concentration in the feed and permeate. No further focus was given to this potential adsorption onto the experimental setup as it was out of the scope of the current study. Therefore, the passage of naproxen at 60 mM $MgCl_2$ and NaCl were excluded from the results (Fig. 5). However, as described in the upcoming paragraphs, no clear trends were observed in the passage of naproxen for different dominant salt ions.

Atenolol and atrazine passage increased by respectively ∼10% and ∼4% in the presence of NaCl at an ionic strength of 60 mM (Fig. 5). Even though a slight increase in the passage of neutral atrazine was observed, no change in PEG passage in the presence of 60 mM NaCl was observed. Therefore, it was assumed that no significant changes in the solute-to-pore size ratio occurred due to an increase in the salinity of the feed solution. Both an increase in atenolol passage and reduced sulfamethoxazole passage were observed, which could potentially be explained by electrostatic screening by NaCl [72]. In the presence of Na_2SO_4, the passage of sulfamethoxazole increased from 19 ± 2% to 35 ± 4%, while the passage of atenolol was slightly reduced from 7 ± 1% to 4.5 ± 0.2% at 60 mM ionic strength (Fig. 5). These altered passages show a similar but lessened change as observed with the dNF80 membrane, indicating the potential occurrence of similar electrostatic interactions as described in the previous section. No changes in atrazine passage due to Na_2SO_4 were observed (Fig. 5). Since atrazine is a neutral substance under the current experimental conditions, this observation was in line with its expected behaviour. Lastly, the passage of naproxen did not seem to be affected by the presence of Na_2SO_4.

$MgCl_2$ led to a decreased passage of sulfamethoxazole, while atenolol passage increased. A decrease from 19 ± 2% to 9 ± 0.2% in sulfamethoxazole passage was observed, which is in line with the expected effect of ion transport induced transmembrane electric field slowing down the passage of negatively charged solutes [73]. The

passage of positively charged MPs, i.e. atenolol, is consequently enhanced, increasing from $7 \pm 1\%$ to $14 \pm 1\%$. Similar to the results gathered with Na_2SO_4, no apparent effect of the dominant ions on the passage of naproxen was observed. A slight drop in naproxen passage was observed at 15 mM ionic strength, after which the passage increased within the standard error of the passage without the presence of ions. Therefore, it was not possible to predict naproxens' behaviour based on the current experimental results. Atrazine passage again was not affected by the presence of $MgCl_2$, indicating no changes in the membrane pore size due to salt at increasing ionic strengths.

Clearly, dominant salts can influence the passage of charged MPs through NF membranes. Most trends can be qualitatively explained based on the proposed theory by Yaroshchuk [73]. To further explore the observed mechanisms and discuss the results more in-depth, the commonly used DSPM-DE transport model will be applied in the following section.

4.4. Modelling

In this section, we use a modified version of the well-known DSPM&DE model to qualitatively interpret the experimentally observed MP passage in the presence of different salts (NaCl, $MgCl_2$ and Na_2SO_4) at increasing ionic strength.

As a first step, both membranes are characterised based on a set of filtration measurements. This includes pure water permeability and PEG retention measurements to quantify the steric exclusion mechanism of both membranes (determination of a representative pore size distribution). Since both the passage of atrazine as well as the passage of diethylene glycol (SI3) did not show a significant dependency on ionic strength, the pore size distribution was assumed to be constant under all conditions. The initial assumption of charge-based properties independent of salt type and concentration led to poor predictions of MP and ternary ion passage (more details provided in SI4 and SI5). Therefore, accounting for salt-specific properties when quantifying charge-based membrane properties (effective membrane charge and dielectric constant) was deemed crucial. Salt-specific but concentration-independent dielectric properties of the membranes were derived based on ternary ion retention measurements, as proposed by [67]. Respective effective charge densities of the membranes (dependent on salt concentration) were fitted to salt passage determined during the MP passage measurements. The fitted membrane parameters, presented in SI6, are then kept constant in the following.

We want to illustrate that the dependency of charge-based membrane fitting parameters in the DSPM&DE model on ionic solution composition is indeed not unexpected and has multiple potential causes. The variation of effective charge density [44,74–77] and effective dielectric constant [44,75,76] in modelling of ion transport through NF membranes when using the DSPM&DE model are frequently observed. This phenomenon is equivalent to observations by Bason et al. [78], where ideal Donnan exclusion fails to explain observed trends in salt permeability with salt concentration. The commonly used DSPM&DE model does not account for concentration-dependent properties of the membrane. To compensate for this, fitting parameters are determined as a function of salt concentration and type. Causes for observed concentration-dependent fitting parameters that have been discussed are ion adsorption/charge regulation [44,74,75,77], charge screening [75] and ion association [78,79]. The potential relevance of ion association in NF membranes has recently been stressed by Freger [79], who addressed the fundamental flaws of current transport models, eventually causing the need for a large number of parameters since exact mechanisms are not fully understood. Accounting for the exact mechanism of effective charge variation goes beyond the scope of this work and is rather determined by fitting membrane properties to salt passage measurements at varying concentrations. Regarding the fitted effective dielectric constant, a strong dependency on salt type is typically observed in contrast to salt concentration [75,76]. In

these studies, the lower effective dielectric constant in the presence of divalent cations, as observed in this study, was explained by the stronger ordering of adjacent water molecules. While the fitted effective membrane charge density is assumed to represent the charge of the membrane qualitatively, the physical relevance, especially quantitatively, is still questionable. Furthermore, since the parameters for dielectric constant and charge density are negatively correlated for a single salt in the DSPM&DE model, certain trends in parameters could be misleading.

Based on the fitted membrane parameters and the diffusion coefficients of the MPs, the model does not accurately predict the passage of MPs in the presence of 15 mM NaCl for both membranes. An additional affinity parameter was introduced to account for potential specific interactions between MPs and membrane (previously observed in other studies [49,62]). This affinity parameter is obtained by fitting the model to MP passage measurements in the presence of NaCl at an ionic strength of 15 mM, and is assumed to be independent of salt concentration and type (see SI7). Preliminary results on the adsorption behaviour of MPs on both membranes in the presence of different salts indicate a decrease in charge-based interactions independent of salt type, which could be caused by charge screening. Therefore, the affinity parameter is kept constant to limit the amount of data fitting.

Before comparing the model results to experimental observations, we want to provide the necessary theoretical background of electrostatic coupling as discussed by Yaroshchuk [58,59,73].

In the case of a dominant divalent cation with lower permeability than the dominant anion (here Mg^{2+}, which has a passage of about 20% in the presence of Cl^-), the passage of a negative trace ion (i.e. naproxen) is decreased while the passage of a positive trace ion (i.e. atenolol) is increased. Passage of trace ions changes oppositely in the presence of a dominant divalent anion with lower permeability than the dominant cation (i.e. SO_4^{2-}, which has a passage of about 5% in the presence of Na^+).

For a monovalent dominant salt (i.e. NaCl), the change in trace ion passage, again, depends on the ion that is determining the salt passage (typically Cl^- for a negatively charged membrane). While the effects in these three cases are similar, the influence of the latter case will be much smaller compared to the cases of dominant divalent ions.

The extent of the mentioned phenomena is further determined by the permeability of the trace ion through the membrane. A more permeable MP will display a larger variation in passage. A good estimate of the permeability of an MP is the passage with no added salt. For the dNF40 membrane, the passage of the studied MPs is below 20%, meaning the permeability is relatively low. The theoretically predicted influence of the dominant salts on the passage of MPs is much less when compared to the influence on monovalent ions (Na^+/Cl^-). Considering this, no passage exceeding 1 (i.e. negative retention) is expected to occur for the MPs in the current study.

While somewhat superficial, the explanation of the qualitative influence of a dominant salt on trace ion passage via electrostatic coupling suffices for understanding the theoretically predicted results. The interplay of multi-component solutions is complex and depends on many factors, such as membrane flux, membrane charge and ion concentration, which are discussed in much more detail in [73]. In the following, we compare the theoretical and experimental results to evaluate the validity of the DPSM&DE model for predicting MP passage while simultaneously obtaining a qualitative understanding of the electrostatic coupling between MPs and dominant salt.

4.4.1. dNF80

In Fig. 6, we compare the theoretical and experimental passage of MPs using the dNF80 membrane. Here, the sensitivity to the effective dielectric constant (± 3 for NaCl, ± 2 for $MgCl_2$, and ± 5 for Na_2SO_4) is displayed by means of shaded areas in Fig. 6. Since charge-based parameters could not be determined unambiguously in the presence of Na_2SO_4, it was assumed that the dielectric constant is similar to
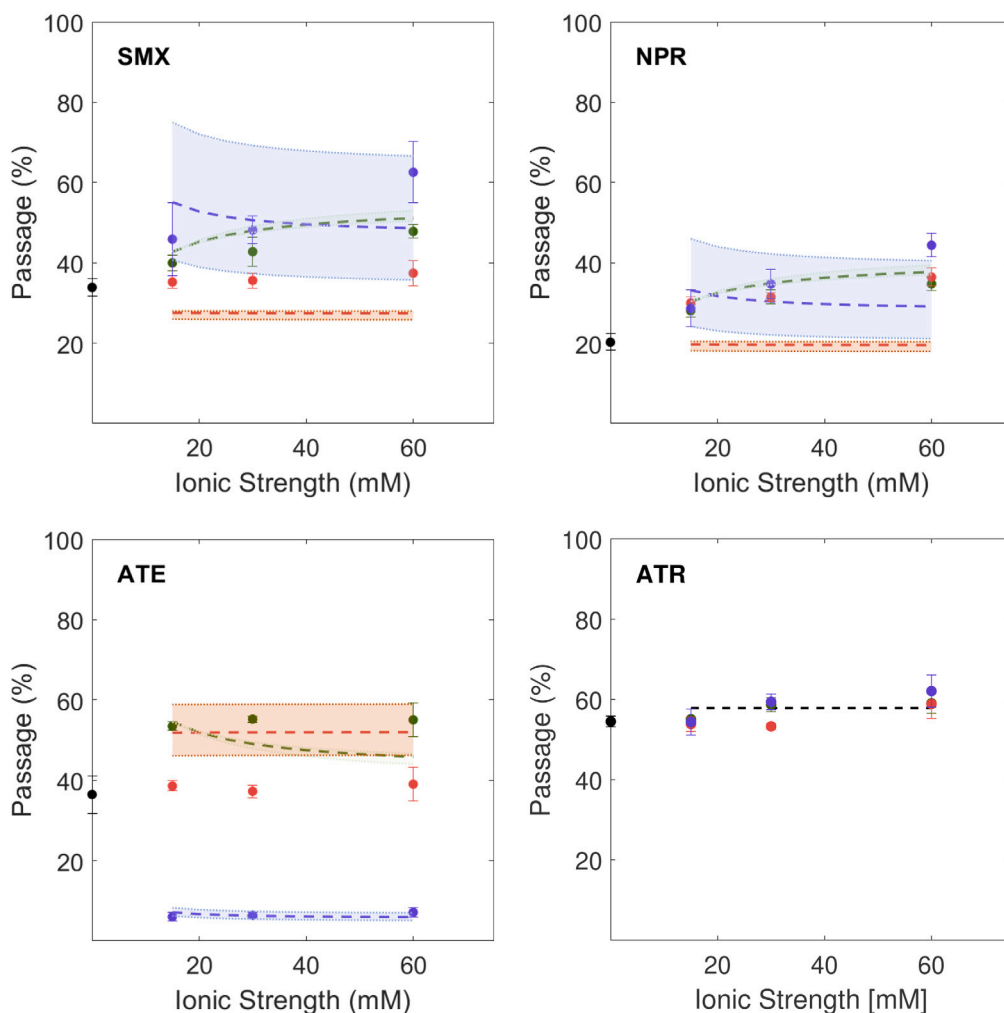
Fig. 6. Influence of increasing ionic strength on passage of MPs through dNF80 membranes predicted by the theoretical transport model. SMX: sulfamethoxazole (−), NPR: naproxen (−), ATE: atenolol (+), ATR: atrazine (0). The black dot at 0 mM ionic strength displays the passage of MPs in pure water as a reference. The dashed lines represent the model prediction for NaCl (green), Na_2SO_4 (blue) and $MgCl_2$ (red). Shaded areas display sensitivity of passage towards estimated charge-based membrane parameters (dielectric constant variation ±3 for NaCl, ±2 for $MgCl_2$ and ±5 for Na_2SO_4). Error bars represent the standard error of each experiment. (For interpretation of the references to colour in this figure legend, the reader is referred to the web version of this article.)

the one in the presence of NaCl. We hypothesise that the influence of counter-ions (i.e. cations) on membrane parameters is more severe, as the concentration inside the membrane is higher due to electrostatic attraction. The sensitivity to effective membrane charge was also evaluated, as shown in SI8. The sensitivity estimated based on confidence intervals of fitted parameters behaves very similarly in both cases, again displaying the coupled nature of these two parameters.

The model does not predict any influence of salt on the passage of atrazine through the dNF80 membrane. This agrees with the experimentally observed passage with an average of 53–62% in all cases. This variation is partially caused by changes in osmotic pressure since those passage values were measured at constant applied pressure. Here, the variations in flux range from 18 to 25 LMH. In diffusion-dominated solute transport processes through NF membranes, the passage increases with decreasing flux.

The unexpected lower variation in passage of sulfamethoxazole and naproxen in the presence of different salts when using the dNF80 compared to the dNF40 membrane (see Fig. 7), is predicted by the model. Considering the electrostatic coupling effect, this is counter-intuitive as the general rule of thumb set previously is that the influence of dominant salt on trace compound would be higher at greater mobility of the trace compound. This is a direct result of the variation in membrane charge depending on the type and concentration of salt

present (relatively large negative charge decreases passage of negative MPs with Na_2SO_4 and less negative charge increases passage of negative MPs with $MgCl_2$). This counteracts the electrostatic coupling effects (increase in passage with Na_2SO_4 and decrease in passage with $MgCl_2$). Trends in the variation of passage with ionic strength are not well described, though, and passage in the presence of $MgCl_2$ is underestimated.

The model predicts the variation in passage of atenolol in the presence of Na_2SO_4 well. In this case, a major influence of the dominant salt on MP passage is observed (passage drops from around 50% to 6%). However, the passage of atenolol in the presence of $MgCl_2$ is overestimated.

Overall, the model describes experimental observations with the dNF80 membrane qualitatively. However, the extent of passage variation for charged MPs in the presence of $MgCl_2$ is consistently overpredicted.

4.4.2. dNF40

The predicted passage of MPs in the presence of a dominant salt is compared to the experimental observations for the dNF40 membrane (Fig. 7). Again, a conservative estimation of parameter deviation is used to determine the sensitivity of the model prediction to these parameters to account for potential errors in the estimation of charge-based membrane parameters. The sensitivity of the model prediction to
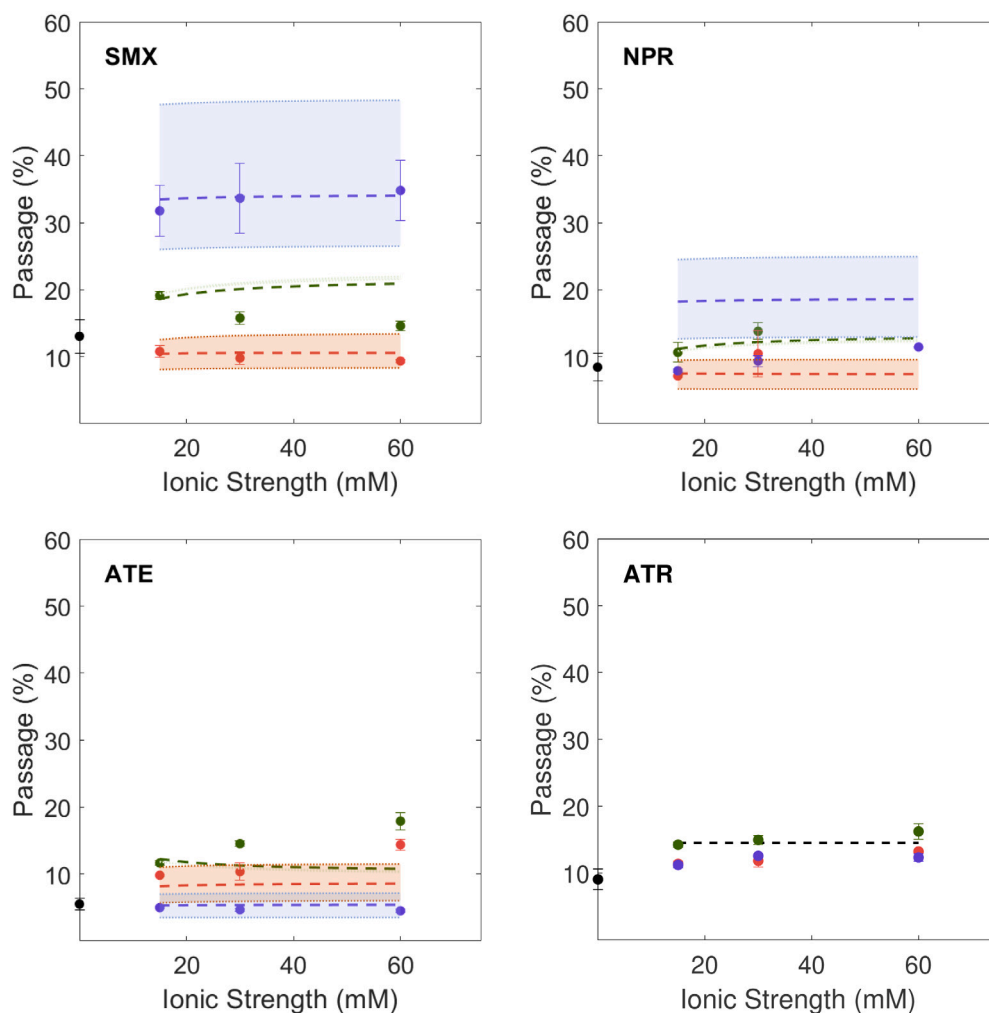
Fig. 7. Influence of increasing ionic strength on passage of MPs through dNF40 membranes predicted by the theoretical transport model. SMX: sulfamethoxazole (−), NPR: naproxen (−), ATE: atenolol (+), ATR: atrazine (0). The black dot at 0 mM ionic strength displays the passage of MPs in pure water as a reference. The dashed lines represent the model prediction for NaCl (green), Na_2SO_4 (blue) and $MgCl_2$ (red). Shaded areas display sensitivity of passage towards estimated charge-based membrane parameters (dielectric constant variation ±3 for NaCl and $MgCl_2$ and ±5 for Na_2SO_4). Error bars represent the standard error of each experiment. (For interpretation of the references to colour in this figure legend, the reader is referred to the web version of this article.)

the effective dielectric constant is displayed by means of shaded areas in Fig. 7. Sensitivity towards effective membrane charge is shown in SI8.

Under the studied conditions, atrazine is uncharged. Therefore, the model does not predict any influence of salts on the passage of atrazine. This corresponds well to the experimentally observed passage with an average of around 11–15% in all cases.

For sulfamethoxazole and naproxen, the model predicts a similar qualitative behaviour with less variation in passage for naproxen. This is due to the fact that naproxen is less mobile (lower passage) than sulfamethoxazole and is, therefore, less affected by the membrane potential. The influence of dominant salt is, despite the large uncertainty in charge-based parameters in the presence of Na_2SO_4, surprisingly well predicted for sulfamethoxazole. For naproxen, variation in passage is overpredicted. Here, no clear trend can be observed in the experimental results.

The passage of atenolol is barely affected by the presence of $MgCl_2$, which the model also predicts. In the presence of Na_2SO_4 the passage decreases from 9% to 6% (a relative decrease of permeate concentration of about 30%), again surprisingly well predicted by the model.

It should be mentioned that model predictions account for both electrostatic coupling and membrane charge variation due to the dominant salt. The variation in charge counteracts the effects of electrostatic coupling for $MgCl_2$ and atenolol (less negative membrane charge decreases

passage of atenolol, while electrostatic coupling increases passage). This is also the reason for the poor prediction of MP retention when not accounting for membrane charge variation.

Overall, the model gives valuable insight into the transport processes of MPs in NF membranes and highlights the relevance of membrane charge and electrostatic coupling caused by dominant salt ions. Although, in most cases, the model qualitatively predicts observed MP removal behaviour, the model is not able to quantitatively predict MP passage with sufficient accuracy. For neutral molecules with no variation expected and observed, the model properly predicts the passage. For charged MPs things become much more complex due to clear electrostatic coupling between MPs and ions while simultaneously being affected by the variation in membrane properties. To properly predict these phenomena, the model has to account for two important aspects. Firstly, charge-based membrane properties have to be accurately determined. This can be done by fitting to retention measurements at varying ionic compositions. A fundamental understanding of the cause for effective membrane property variations could reduce the extensive amount of experiments required and allow for fully predictive model approaches. Secondly, one has to describe both the partitioning and mobility of MPs inside the membrane correctly. Ideally, parameters such as the affinity introduced here should be determined more accurately using separate experimental methods to determine the physical

relevance of this parameter. Although no dependency of affinity on the salt type was indicated in this study, one necessary variation to the model could be implementing a salt-dependent affinity constant. To not fully lose prediction capability by introducing another fitting parameter, further studies investigating these effects more fundamentally are recommended.

5. Conclusion

In this work, we show that dominant salts influence MP removal by hollow fiber NF membranes due to multiple factors. The change in MP removal depends on the type and charge of the MP, the type of dominant salt, and the type of NF membrane used. In this study, two commercially available NF membranes, namely the dNF80 and dNF40, were used. The lower nominal MWCO of the dNF40 membrane resulted in an overall higher MP removal (>85%) and lessened influence of electrostatic coupling to salt flux on MP transport. Experimental results suggest that MP transport through NF membranes is substantially affected by the electrostatic coupling of dominant salts and trace MPs. While the passage of uncharged MPs remained unaffected, substantial changes in the passage of charged MPs in the presence of dominant salts were observed. Such a change was clearly observed for atenolol through the dNF80 membrane, where passage decreased from 36% to 6% in the presence of $5\,mM$ Na_2SO_4. Furthermore, varying the type of membrane reveals that the influence of salts is partially related to the mobility of the MP inside the membrane. It was observed that higher passage of MPs through NF membranes under standard conditions led to an increased influence of dominant salts. To further assist the interpretation of experimental observations, a theoretical transport model (DSPM&DE) was applied. Valuable insight was gained on the importance of both electrostatic coupling of ions and MPs, as well as the influence of ions on charged MP transport caused by a dependency of membrane properties (dielectric constant and charge) on solution composition. The results revealed that, in certain cases, these two effects counterbalance each other, leading to a reduced influence of salt on MP passage than expected for each phenomenon individually. The results show the importance of the ionic background of the feed water on the removal of MPs by NF membranes. Since substantial differences exist between water sources, acquiring sufficient information on the (ionic) water matrix is crucial before estimating the removal of MPs during nanofiltration.

CRediT authorship contribution statement

Sam B. Rutten: Methodology, Conceptualization, Investigation, Formal analysis, Writing – original draft. **Moritz A. Junker:** Methodology, Conceptualization, Investigation, Formal analysis, Writing – original draft. **Lucía Hernández Leal:** Review & editing. **Wiebe M. de Vos:** Review & editing. **Rob G.H. Lammertink:** Review & editing. **Joris de Grooth:** Review & editing.

Declaration of competing interest

The authors declare the following financial interests/personal relationships which may be considered as potential competing interests: Dr. J de Grooth currently holds a position at NX Filtration B.V., a membrane manufacturer. The other authors declare that they have no known competing financial interests or personal relationships that could have appeared to influence the work reported in this paper.

Data availability

Data will be made available on request.

Appendix A. Supplementary data

Supplementary material related to this article can be found online at https://doi.org/10.1016/j.memsci.2023.121625.

References

[1] N.D. Bedding, A.E. McIntyre, R. Perry, J.N. Lester, Organic contaminants in the aquatic environment I. Sources and occurrence, Sci. Total Environ. 25 (2) (1982) 143–167, http://dx.doi.org/10.1016/0048-9697(82)90083-3.

[2] M.O. Barbosa, N.F.F. Moreira, A.R. Ribeiro, M.F.R. Pereira, A.M.T. Silva, Occurrence and removal of organic micropollutants: An overview of the watch list of EU decision 2015/495, Water Res. 94 (2016) 257–279, http://dx.doi.org/10.1016/j.watres.2016.02.047.

[3] A. Butkovskyi, L.H. Leal, G. Zeeman, H.H.M. Rijnaarts, Micropollutants in source separated wastewater streams and recovered resources of source separated sanitation, Environ. Res. 156 (2017) 434–442, http://dx.doi.org/10.1016/j.envres.2017.03.044.

[4] A. Egea-Corbacho, S. Gutiérrez Ruiz, J.M. Quiroga Alonso, Removal of emerging contaminants from wastewater using nanofiltration for its subsequent reuse: Full–scale pilot plant, J. Cleaner Prod. 214 (2019) 514–523, http://dx.doi.org/10.1016/j.jclepro.2018.12.297.

[5] E. Eriksson, K. Auffarth, A.M. Eilersen, M. Henze, A. Ledin, Household chemicals and personal care products as sources for xenobiotic organic compounds in grey wastewater, Water SA 29 (2) (2003) 135–146, http://dx.doi.org/10.4314/wsa.v29i2.4848.

[6] Y. Luo, W. Guo, H.H. Ngo, L.D. Nghiem, F.I. Hai, J. Zhang, S. Liang, X.C. Wang, A review on the occurrence of micropollutants in the aquatic environment and their fate and removal during wastewater treatment, Sci. Total Environ. 473–474 (2014) 619–641, http://dx.doi.org/10.1016/j.scitotenv.2013.12.065.

[7] R.P. Schwarzenbach, B.I. Escher, K. Fenner, T.B. Hofstetter, C.A. Johnson, U. von Gunten, B. Wehrli, The challenge of micropollutants in aquatic systems, Science 313 (5790) (2006) 1072–1077, http://dx.doi.org/10.1126/science.1127291.

[8] R. Tröger, P. Klöckner, L. Ahrens, K. Wiberg, Micropollutants in drinking water from source to tap - method development and application of a multiresidue screening method, Sci. Total Environ. 627 (2018) 1404–1432, http://dx.doi.org/10.1016/j.scitotenv.2018.01.277.

[9] N.G.F.M. van der Aa, E. Dijkman, L. Bijlsma, E. Emke, B.M. van de Ven, A.L.N. van Nuijs, P. de Voogt, Drugs of Abuse and Tranquilizers in Dutch Surface Waters, Drinking Water and Wastewater - Results of Screening Monitoring 2009, National Institute for Public Health and the Environment, 2010.

[10] M. Schriks, M.B. Heringa, M.M.E. van der Kooi, P. de Voogt, A.P. van Wezel, Toxicological relevance of emerging contaminants for drinking water quality, Water Res. 44 (2) (2010) 461–476, http://dx.doi.org/10.1016/j.watres.2009.08.023.

[11] R. Loos, B.M. Gawlik, G. Locoro, E. Rimaviciute, S. Contini, G. Bidoglio, EU-wide survey of polar organic persistent pollutants in European river waters, Environ. Pollut. 157 (2) (2009) 561–568, http://dx.doi.org/10.1016/j.envpol.2008.09.020.

[12] P.d. Voogt, M.-L. Janex-Habibi, F. Sacher, L. Puijker, M. Mons, Development of a common priority list of pharmaceuticals relevant for the water cycle, Water Sci. Technol. 59 (1) (2009) 39–46, http://dx.doi.org/10.2166/wst.2009.764.

[13] S.A. Snyder, P. Westerhoff, Y. Yoon, D.L. Sedlak, Pharmaceuticals, personal care products, and endocrine disruptors in water: Implications for the water industry, Environ. Eng. Sci. 20 (5) (2003) 449–469, http://dx.doi.org/10.1089/109287503768335931.

[14] World Health Organization, Drinking-Water, World Health Organization, 2019, URL https://www.who.int/news-room/fact-sheets/detail/drinking-water.

[15] UNESCO, WWAP (united nations world water assessment programme). The united nations world water development report 2017. Wastewater: The untapped resource, 2017.

[16] World Health Organization, Potable reuse: Guidance for producing safe drinking-water, 2017.

[17] N.K. Khanzada, M.U. Farid, J.A. Kharraz, J. Choi, C.Y. Tang, L.D. Nghiem, A. Jang, A.K. An, Removal of organic micropollutants using advanced membrane-based water and wastewater treatment: A review, J. Membr. Sci. 598 (2020) 117672, http://dx.doi.org/10.1016/j.memsci.2019.117672.

[18] C. Bellona, J.E. Drewes, G. Oelker, J. Luna, G. Filteau, G. Amy, Comparing nanofiltration and reverse osmosis for drinking water augmentation, J. AWWA 100 (9) (2008) 102–116, http://dx.doi.org/10.1002/j.1551-8833.2008.tb09724.x.

[19] J. Radjenović, M. Petrović, F. Ventura, D. Barceló, Rejection of pharmaceuticals in nanofiltration and reverse osmosis membrane drinking water treatment, Water Res. 42 (14) (2008) 3601–3610, http://dx.doi.org/10.1016/j.watres.2008.05.020.

[20] A. Verliefde, E. Cornelissen, G. Amy, B. van der Bruggen, H. van Dijk, Priority organic micropollutants in water sources in Flanders and the Netherlands and assessment of removal possibilities with nanofiltration, Environ. Pollut. 146 (1) (2007) 281–289, http://dx.doi.org/10.1016/j.envpol.2006.01.051.

[21] B. Van der Bruggen, C. Vandecasteele, Removal of pollutants from surface water and groundwater by nanofiltration: overview of possible applications in the drinking water industry, Environ. Pollut. 122 (3) (2003) 435–445, http://dx.doi.org/10.1016/S0269-7491(02)00308-1.

[22] M. Taheran, S.K. Brar, M. Verma, R.Y. Surampalli, T.C. Zhang, J.R. Valero, Membrane processes for removal of pharmaceutical active compounds (PhACs) from water and wastewaters, Sci. Total Environ. 547 (2016) 60–77, http://dx.doi.org/10.1016/j.scitotenv.2015.12.139.

[23] C.-H. Wei, N. Wang, C. HoppeJones, T. Leiknes, G. Amy, Q. Fang, X. Hu, H. Rong, Organic micropollutants removal in sequential batch reactor followed by nanofiltration from municipal wastewater treatment, Bioresour. Technol. 268 (2018) 648–657, http://dx.doi.org/10.1016/j.biortech.2018.08.073.

[24] J. Garcia-Ivars, L. Martella, M. Massella, C. Carbonell-Alcaina, M.-I. Alcaina-Miranda, M.-I. Iborra-Clar, Nanofiltration as tertiary treatment method for removing trace pharmaceutically active compounds in wastewater from wastewater treatment plants, Water Res. 125 (2017) 360–373, http://dx.doi.org/10.1016/j.watres.2017.08.070.

[25] A. Azaïs, J. Mendret, S. Gassara, E. Petit, A. Deratani, S. Brosillon, Nanofiltration for wastewater reuse: Counteractive effects of fouling and matrice on the rejection of pharmaceutical active compounds, Sep. Purif. Technol. 133 (2014) 313–327, http://dx.doi.org/10.1016/j.seppur.2014.07.007.

[26] K. Kimura, G. Amy, J.E. Drewes, T. Heberer, T.-U. Kim, Y. Watanabe, Rejection of organic micropollutants (disinfection by-products, endocrine disrupting compounds, and pharmaceutically active compounds) by NF/RO membranes, J. Membr. Sci. 227 (1) (2003) 113–121, http://dx.doi.org/10.1016/j.memsci.2003.09.005.

[27] R. Xu, P. Zhang, Q. Wang, X. Wang, K. Yu, T. Xue, X. Wen, Influences of multi influent matrices on the retention of PPCPs by nanofiltration membranes, Sep. Purif. Technol. 212 (2019) 299–306, http://dx.doi.org/10.1016/j.seppur.2018.11.040.

[28] Y. Wang, I. Zucker, C. Boo, M. Elimelech, Removal of emerging wastewater organic contaminants by polyelectrolyte multilayer nanofiltration membranes with tailored selectivity, ACS ES&T Eng. (2020) http://dx.doi.org/10.1021/acsestengg.0c00160.

[29] E. te Brinke, D.M. Reurink, I. Achterhuis, J. de Grooth, W.M. de Vos, Asymmetric polyelectrolyte multilayer membranes with ultrathin separation layers for highly efficient micropollutant removal, Appl. Mater. Today (2019) 100471, http://dx.doi.org/10.1016/j.apmt.2019.100471.

[30] S.M. Abtahi, S. Ilyas, C. Joannis Cassan, C. Albasi, W.M. de Vos, Micropollutants removal from secondary-treated municipal wastewater using weak polyelectrolyte multilayer based nanofiltration membranes, J. Membr. Sci. 548 (2018) 654–666, http://dx.doi.org/10.1016/j.memsci.2017.10.045.

[31] S. Ilyas, S.M. Abtahi, N. Akkilic, H.D.W. Roesink, W.M. de Vos, Weak polyelectrolyte multilayers as tunable separation layers for micro-pollutant removal by hollow fiber nanofiltration membranes, J. Membr. Sci. 537 (2017) 220–228, http://dx.doi.org/10.1016/j.memsci.2017.05.027.

[32] T.-Y. Liu, L.-X. Bian, H.-G. Yuan, B. Pang, Y.-K. Lin, Y. Tong, B. Van der Bruggen, X.-L. Wang, Fabrication of a high-flux thin film composite hollow fiber nanofiltration membrane for wastewater treatment, J. Membr. Sci. 478 (2015) 25–36, http://dx.doi.org/10.1016/j.memsci.2014.12.029.

[33] J.d. Grooth, D.M. Reurink, J. Ploegmakers, W.M.d. Vos, K. Nijmeijer, Charged micropollutant removal with hollow fiber nanofiltration membranes based on polycation/polyzwitterion/polyanion multilayers, ACS Appl. Mater. Interfaces 6 (19) (2014) 17009–17017, http://dx.doi.org/10.1021/am504630a.

[34] A.W. Mohammad, Y.H. Teow, W.L. Ang, Y.T. Chung, D.L. Oatley-Radcliffe, N. Hilal, Nanofiltration membranes review: Recent advances and future prospects, Desalination 356 (2015) 226–254, http://dx.doi.org/10.1016/j.desal.2014.10.043.

[35] R.W. Baker, Membrane Technology and Applications, third ed., John Wiley & Sons, 2012, pp. 222–224.

[36] E. te Brinke, I. Achterhuis, D.M. Reurink, J. de Grooth, W.M. de Vos, Multiple approaches to the buildup of asymmetric polyelectrolyte multilayer membranes for efficient water purification, ACS Appl. Polym. Mater. 2 (2) (2020) 715–724, http://dx.doi.org/10.1021/acsapm.9b01038.

[37] D.M. Reurink, E. te Brinke, I. Achterhuis, H.D.W. Roesink, W.M. de Vos, Nafion-based low-hydration polyelectrolyte multilayer membranes for enhanced water purification, ACS Appl. Polym. Mater. 1 (9) (2019) 2543–2551, http://dx.doi.org/10.1021/acsapm.9b00689.

[38] T.-Y. Liu, Z.-H. Liu, R.-X. Zhang, Y. Wang, B.V.d. Bruggen, X.-L. Wang, Fabrication of a thin film nanocomposite hollow fiber nanofiltration membrane for wastewater treatment, J. Membr. Sci. 488 (2015) 92–102, http://dx.doi.org/10.1016/j.memsci.2015.04.020.

[39] L.D. Nghiem, A.I. Schäfer, M. Elimelech, Removal of natural hormones by nanofiltration membranes: Measurement, modeling, and mechanisms, Environ. Sci. Technol. 38 (6) (2004) 1888–1896, http://dx.doi.org/10.1021/es034952r.

[40] Y. Kiso, A. Mizuno, R.A.A.b. Othman, Y.-J. Jung, A. Kumano, A. Ariji, Rejection properties of pesticides with a hollow fiber NF membrane (HNF-1), Desalination 143 (2) (2002) 147–157, http://dx.doi.org/10.1016/S0011-9164(02)00236-9.

[41] A.I. Cavaco Morão, A. Szymczyk, P. Fievet, A.M. Brites Alves, Modelling the separation by nanofiltration of a multi-ionic solution relevant to an industrial process, J. Membr. Sci. 322 (2) (2008) 320–330, http://dx.doi.org/10.1016/j.memsci.2008.06.003.

[42] S. Déon, P. Dutournié, L. Limousy, P. Bourseau, Transport of salt mixtures through nanofiltration membranes: Numerical identification of electric and dielectric contributions, Sep. Purif. Technol. 69 (3) (2009) 225–233, http://dx.doi.org/10.1016/j.seppur.2009.07.022.

[43] O. Labban, C. Liu, T.H. Chong, J.H. Lienhard V, Fundamentals of low-pressure nanofiltration: Membrane characterization, modeling, and understanding the multi-ionic interactions in water softening, J. Membr. Sci. 521 (2017) 18–32, http://dx.doi.org/10.1016/j.memsci.2016.08.062.

[44] V. Silva, V. Geraldes, A.M. Brites Alves, L. Palacio, P. Prádanos, A. Hernández, Multi-ionic nanofiltration of highly concentrated salt mixtures in the seawater range, Desalination 277 (1) (2011) 29–39, http://dx.doi.org/10.1016/j.desal.2011.03.088.

[45] A.H.M.A. Sadmani, R.C. Andrews, D.M. Bagley, Impact of natural water colloids and cations on the rejection of pharmaceutically active and endocrine disrupting compounds by nanofiltration, J. Membr. Sci. 450 (2014) 272–281, http://dx.doi.org/10.1016/j.memsci.2013.09.017.

[46] R. Boussahel, A. Montiel, M. Baudu, Effects of organic and inorganic matter on pesticide rejection by nanofiltration, Desalination 145 (1) (2002) 109–114, http://dx.doi.org/10.1016/S0011-9164(02)00394-6.

[47] L.D. Nghiem, S. Hawkes, Effects of membrane fouling on the nanofiltration of pharmaceutically active compounds (PhACs): Mechanisms and role of membrane pore size, Sep. Purif. Technol. 57 (1) (2007) 176–184, http://dx.doi.org/10.1016/j.seppur.2007.04.002.

[48] A. Verliefde, E. Cornelissen, S. Heijman, J.Q.J.C. Verberk, G. Amy, B. Van der Bruggen, J. Dijk, The role of electrostatic interactions on the rejection of organic solutes in aqueous solutions with nanofiltration, J. Membr. Sci. 322 (2008) 52–66, http://dx.doi.org/10.1016/j.memsci.2008.05.022.

[49] A.R.D. Verliefde, E.R. Cornelissen, S.G.J. Heijman, J.Q.J.C. Verberk, G.L. Amy, B. Van der Bruggen, J.C. van Dijk, Construction and validation of a full-scale model for rejection of organic micropollutants by NF membranes, J. Membr. Sci. 339 (1) (2009) 10–20, http://dx.doi.org/10.1016/j.memsci.2009.03.038.

[50] K. Wesolowska, S. Koter, M. Bodzek, Modelling of nanofiltration in softening water, Desalination 162 (2004) 137–151, http://dx.doi.org/10.1016/S0011-9164(04)00037-2.

[51] L. Flyborg, B. Björlenius, M. Ullner, K.M. Persson, A PLS model for predicting rejection of trace organic compounds by nanofiltration using treated wastewater as feed, Sep. Purif. Technol. 174 (2017) 212–221, http://dx.doi.org/10.1016/j.seppur.2016.10.029.

[52] E.R. Cornelissen, J. Verdouw, A.J. Gijsbertsen-Abrahamse, J.A.M.H. Hofman, A nanofiltration retention model for trace contaminants in drinking water sources, Desalination 178 (1) (2005) 179–192, http://dx.doi.org/10.1016/j.desal.2004.11.047.

[53] A.R. Verliefde, S. Heijman, E. Cornelissen, G. Amy, B. Van der Bruggen, J. Van Dijk, Influence of electrostatic interactions on the rejection with NF and assessment of the removal efficiency during NF/GAC treatment of pharmaceutically active compounds in surface water, Water Res. 41 (15) (2007) 3227–3240, http://dx.doi.org/10.1016/j.watres.2007.05.022.

[54] S. Castaño Osorio, P.M. Biesheuvel, E. Spruijt, J.E. Dykstra, A. van der Wal, Modeling micropollutant removal by nanofiltration and reverse osmosis membranes: considerations and challenges, Water Res. 225 (2022) 119130, http://dx.doi.org/10.1016/j.watres.2022.119130.

[55] V. Yangali-Quintanilla, S.K. Maeng, T. Fujioka, M. Kennedy, G. Amy, Proposing nanofiltration as acceptable barrier for organic contaminants in water reuse, J. Membr. Sci. 362 (1) (2010) 334–345, http://dx.doi.org/10.1016/j.memsci.2010.06.058.

[56] K. Plakas, A. Karabelas, Membrane retention of herbicides from single and multi-solute media: The effect of ionic environment, J. Membr. Sci. 320 (2008) 325–334, http://dx.doi.org/10.1016/j.memsci.2008.04.016.

[57] L. Yang, J. Zhou, Q. She, M.P. Wan, R. Wang, V.W.C. Chang, C.Y. Tang, Role of calcium ions on the removal of haloacetic acids from swimming pool water by nanofiltration: mechanisms and implications, Water Res. 110 (2017) 332–341, http://dx.doi.org/10.1016/j.watres.2016.11.040.

[58] A. Yaroshchuk, X. Martínez-Lladó, L. Llenas, M. Rovira, J. de Pablo, Solution-diffusion-film model for the description of pressure-driven trans-membrane transfer of electrolyte mixtures: One dominant salt and trace ions, J. Membr. Sci. 368 (1) (2011) 192–201, http://dx.doi.org/10.1016/j.memsci.2010.11.037.

[59] N. Pages, A. Yaroshchuk, O. Gibert, J.L. Cortina, Rejection of trace ionic solutes in nanofiltration: Influence of aqueous phase composition, Chem. Eng. Sci. 104 (2013) 1107–1115, http://dx.doi.org/10.1016/j.ces.2013.09.042.

[60] P. Verlicchi, M. Al Aukidy, E. Zambello, Occurrence of pharmaceutical compounds in urban wastewater: Removal, mass load and environmental risk after a secondary treatment—A review, Sci. Total Environ. 429 (2012) 123–155, http://dx.doi.org/10.1016/j.scitotenv.2012.04.028.

[61] C.R. Wilke, P. Chang, Correlation of diffusion coefficients in dilute solutions, AIChE J. 1 (2) (1955) 264–270, http://dx.doi.org/10.1002/aic.690010222.

[62] X.-m. Wang, B. Li, T. Zhang, X.-y. Li, Performance of nanofiltration membrane in rejecting trace organic compounds: Experiment and model prediction, Desalination 370 (2015) 7–16, http://dx.doi.org/10.1016/j.desal.2015.05.010.

[63] M.A. Junker, W.M. de Vos, R.G.H. Lammertink, J. de Groth, Bridging the gap between lab-scale and commercial dimensions of hollow fiber nanofiltration membranes, J. Membr. Sci. 624 (2021) 119100, http://dx.doi.org/10.1016/j.memsci.2021.119100.

[64] M.A. Junker, W.M. de Vos, J. de Groth, R.G.H. Lammertink, Relating uncharged solute retention of polyelectrolyte multilayer nanofiltration membranes to effective structural properties, J. Membr. Sci. 668 (2023) 121164, http://dx.doi.org/10.1016/j.memsci.2022.121164.

[65] A. Szymczyk, P. Fievet, Investigating transport properties of nanofiltration membranes by means of a steric, electric and dielectric exclusion model, J. Membr. Sci. 252 (1–2) (2005) 77–88, http://dx.doi.org/10.1016/j.memsci.2004.12.002.

[66] D.L. Oatley-Radcliffe, S.R. Williams, M.S. Barrow, P.M. Williams, Critical appraisal of current nanofiltration modelling strategies for seawater desalination and further insights on dielectric exclusion, Desalination 343 (2014) 154–161, http://dx.doi.org/10.1016/j.desal.2013.10.001.

[67] S. Déon, A. Escoda, P. Fievet, P. Dutournié, P. Bourseau, How to use a multi-ionic transport model to fully predict rejection of mineral salts by nanofiltration membranes, Chem. Eng. J. 189–190 (2012) 24–31, http://dx.doi.org/10.1016/j.cej.2012.02.014.

[68] S. Bandini, D. Vezzani, Nanofiltration modeling: the role of dielectric exclusion in membrane characterization, Chem. Eng. Sci. 58 (15) (2003) 3303–3326, http://dx.doi.org/10.1016/s0009-2509(03)00212-4.

[69] A.R.D. Verliefde, E.R. Cornelissen, S.G.J. Heijman, E.M.V. Hoek, G.L. Amy, B.V.d. Bruggen, J.C. van Dijk, Influence of solute-membrane affinity on rejection of uncharged organic solutes by nanofiltration membranes, Environ. Sci. Technol. 43 (7) (2009) 2400–2406, http://dx.doi.org/10.1021/es803146r.

[70] V. Geraldes, A.M. Brites Alves, Computer program for simulation of mass transport in nanofiltration membranes, J. Membr. Sci. 321 (2) (2008) 172–182, http://dx.doi.org/10.1016/j.memsci.2008.04.054.

[71] A. Escoda, P. Fievet, S. Lakard, A. Szymczyk, S. Déon, Influence of salts on the rejection of polyethyleneglycol by an NF organic membrane: Pore swelling and salting-out effects, J. Membr. Sci. 347 (1) (2010) 174–182, http://dx.doi.org/10.1016/j.memsci.2009.10.021.

[72] J. Luo, W. Yinhua, Effect of pH and salt on nanofiltration – a critical review, J. Membr. Sci. (2013) http://dx.doi.org/10.1016/j.memsci.2013.03.029.

[73] A.E. Yaroshchuk, Negative rejection of ions in pressure-driven membrane processes, Adv. Colloid Interface Sci. 139 (1) (2008) 150–173, http://dx.doi.org/10.1016/j.cis.2008.01.004.

[74] J. Schaep, C. Vandecasteele, A.W. Mohammad, W.R. Bowen, Analysis of the salt retention of nanofiltration membranes using the donnan–steric partitioning pore model, Sep. Sci. Technol. 34 (15) (1999) 3009–3030, http://dx.doi.org/10.1081/ss-100100819.

[75] S. Déon, A. Escoda, P. Fievet, A transport model considering charge adsorption inside pores to describe salts rejection by nanofiltration membranes, Chem. Eng. Sci. 66 (12) (2011) 2823–2832, http://dx.doi.org/10.1016/j.ces.2011.03.043.

[76] A. Escoda, Y. Lanteri, P. Fievet, S. Déon, A. Szymczyk, Determining the dielectric constant inside pores of nanofiltration membranes from membrane potential measurements, Langmuir 26 (18) (2010) 14628–14635, http://dx.doi.org/10.1021/la1023949.

[77] S. Castaño Osorio, P.M. Biesheuvel, J.E. Dykstra, E. Virga, Nanofiltration of complex mixtures: The effect of the adsorption of divalent ions on membrane retention, Desalination 527 (2022) 115552, http://dx.doi.org/10.1016/j.desal.2022.115552.

[78] S. Bason, V. Freger, Phenomenological analysis of transport of mono- and divalent ions in nanofiltration, J. Membr. Sci. 360 (1) (2010) 389–396, http://dx.doi.org/10.1016/j.memsci.2010.05.037.

[79] V. Freger, Ion partitioning and permeation in charged low-T* membranes, Adv. Colloid Interface Sci. 277 (2020) 102107, http://dx.doi.org/10.1016/j.cis.2020.102107.